真空中平行钼丝辐射加热下的6英寸单晶硅基片的温度分布

李帅辉 舒勇华 唐锦荣 樊菁

(中国科学院力学研究所高温气体动力学重点实验室,北京 100080)

摘 要:真空辐射加热下基片表面温度分布的均匀性是薄膜制备中的关键问题之一。本文采用数值计算和比色红外测温两种方法,研究了我们研制的真空辐射加热器(IMCAS-VRH)的性能。利用IMCAS-VRH加热直径6英寸的单晶硅基片,当电功率为3860 W时,基片表面平均温度为1093 K,整个基片上的温度变化的测量值约为6 K。基片表面温度分布的计算结果与测量数据符合得很好,进一步的计算分析表明钼丝对辐射的遮挡效应、隔热屏和基片热传导等对基片温度分布均匀性有重要影响。

关键词:大面积基片;真空辐射加热;温度分布均匀性;比色红外测温;计算分析

Temperature Distribution over 6 - inch Mono - crystal Silicon Substrate Heated by Parallel Molybdenum Filaments in Vacuum

Li Shuaihui Shu Yonghua Tang Jinrong Fan Jing

(Key Laboratory of High Temperature Gas Dynamics, Institute of Mechanics, Chinese Academy of Sciences, Beijing 100080, China)

Abstract: Uniform temperature distribution over a substrate is one of the important issues in the vapor deposition of large - area films. We employ both numerical and experimental approaches to study the temperature distribution over a 6 - inch monocrystal silicon substrate radiated by a molybdenum filament heater in our PVD facility. An infrared colorimetric measurement shows that the mean temperature of the substrate is 1093 K under an electric power of 3860 W, and the maximum temperature difference between the center and circumference is about 6 K. The calculated temperature distributions agree well with the experimental data, and further computational analysis shows that the shielding effect of the molybdenum filaments on radiation, the number of thermal insulation plates around the heater, and the thermal conduction of the heater walls and substrate all affect significantly the substrate temperature distribution. It is therefore needed to consider them in the design of high performance substrate heaters.

Keywords: Large - area Substrate; Radiative Heating in Vacuum; Uniformity of Temperature Distribution; Infrared Colorimetric Measurement of Temperature; Calculational Analysis

1 Introduction

In the process of thin - film vapor deposition, the substrate temperature has an important effect on the adhesion, migration, nucleation and crystallization of incident vapor particles. One of the crucial issues in preparation of large - area thin films is how to generate a uniform temperature distribution over the substrates. There are two means to heat a substrate in vacuum, namely thermal conduction and radiation. The former is convenient and efficient in heating a small - area substrate through the compact contact between the substrate and heater[1-3], while the latter is often preferred in heating large - area substrates to meet the uniform temperature demand[4-9]. Moreover, the radiative heating less pollutes substrate surfaces, and may rotate and change deposition sides in vacuum condition[5,9], which is very important for double sided film deposition.

Some progress has been made towards calculating or measuring. Clark et. al[6] calculated the temperature distribution of the substrate surface in a one - dimensional model, supposing that the surface of the radiative heating cavity was at the same temperature and neglecting the cavity surfaces' reflection and the substrate's thermal conduction. Tsaneva et. al[7] calculated the distribution of radiative heat flux of the substrate surface on the bottom of a closed isothermal radiative cavity. Chen et. al[10] studied the temperature uniformity of the rotating substrate in a isothermal radiative cylinder. Bellman et. al[11] simplified the heating filament as 'line of point sources' when calculating the heat flux and the temperature of the substrate surface, and neglected the impacts of other parts. These models were simplified too much due to the consideration for the convenience in theoretical analysis or calculations, without comparing the calculational results with the experimental results, so they are not fit for guiding the fine design of vacuum radiation heaters for large - area substrates. When it comes to experiments, Geerk et. al[8] measured the temperature uniformity of the surface of a 6 - inch diameter substrate by moving the thermocouple in vacuum. The temperature of the substrate is about 1000 K, the temperature uniformity in the central 5 - inch region is about 5 K, and that in the outboard region increases rapidly to about 25 K. Westerheim et. al[12,13] used a thermocouple to measure the relation between the temperature of the substrate surface and the electric heating power, and employed the bonding of a Au - Pt - Pd thermocouple with a diameter of 25 - μm in order to increase the measurement precision. Choi et. al[14,15] measured the temperature uniformity of the substrate surface in the process of film deposition, using an adaptively calibrated pyrometer, but the precision was highly dependent on the selective parameters of the substrate.

This article calculates the temperature distribution of the surface of a 6 - inch monocrystal silicon substrate radiatively heated in vacuum, and examines the effect of the molybdenum filaments' shielding, the heat shields, the thermal conduction etc. on the temperature uniformity of the

substrate surface. The calculational results of the temperature uniformity accord well with the metrical results by a colorimetric infrared pyrometer. This article has six sections. Section 1 briefly illuminates the configuration of our vacuum radiation heater and the method of using a colorimetric infrared pyrometer to measure the temperature distribution of the substrate surface by moving the substrate in vacuum. In section 2 we calculate the radiative heat flux between the filaments, the heater base, the heater supports, the substrate holder and the substrate by using the surface element method, and calculate the temperature distribution of the substrate surface by using the finite difference method. In section 3 we compare the calculational results of the temperature distribution of the substrate surface with the metrical data, and analyze the effects of various factors on the temperature distribution. The last section is with the concluding remarks.

2 Experimental facility and infrared colorimetric measurement of temperature distribution

As shown in Fig. 1, a radiative heater (RH) is suspended in the vacuum chamber of our PVD facility that has a double - layer wall with cooling water inside. RH consists of twenty - four molybdenum filaments with a diameter of 3 mm, one rectangular standing plate, four side plates, two layers of thin plates for thermal insulation, and one substrate holder (Fig. 1). All the plates are made of 1Cr18Ni9Ti stainless steel. The standing and side plates, together with the substrate and its holder, form a closed rectangular radiative cavity of 200 mm × 200 mm × 22 mm.

The filaments are uniformly arranged in parallel, and the center distance between two neighboring filaments is 8 mm. They horizontally pass through the isolating Al_2O_3 tubes inserted into a couple of supporting plates, and connected each other through metal clamps. The filaments are 10 mm and 12 mm vertically away from the standing plate and substrate, respectively. A Pt/Rh - Pt thermocouple is mounted on the standing plate center to measure and control the local temperature via a thermoregulator.

An infrared colorimetric detector of temperature, named as CIT - 1MD, vertically focuses on a substrate through a quartz glass window centered in the bottom flange (Fig. 1). The heater driven by two stepping motors may move two - dimensionally along slide tracks, and the moving paths are controlled by a computer following the designed trajectories. When the heater moves along the parallel - lines, the detector focus may scan and obtain the temperature distribution over the substrate. An appropriate range for CIT - 1MD to measure temperature is 950 ~ 2000 K, and its response time, space resolution and measurement accuracy are 67 ms, 5 mm and 1 K, respectively.

The emissive power spectrum is given by the Planck formula as follows

$$E(\lambda,T)=\frac{c_1\varepsilon(\lambda,T)\lambda^{-5}}{\exp(c_2/\lambda T)-1}, \qquad (1)$$

where $\varepsilon(\lambda,T)$ is the emissivity, λ is

the wavelength, T is the temperature, and c_1 and c_2 are the first and second radiative constants.

Let:

$B=E(\lambda_1,T_s)/E(\lambda_2,T_s)$

$\chi=\varepsilon(\lambda_1,T_s)/\varepsilon(\lambda_2,T_s)$, then the temperature of the measured surface is of the form

$$T_s=\frac{c_2(\lambda_2^{-1}-\lambda_1^{-1})}{\ln B-\ln\chi-5\ln(\lambda_2/\lambda_1)} \qquad (2)$$

For a nonmetallic monocrystal silicon surface, χ, which is corrected by CIT-1MD, is equal to 0.97. Substituting the values of $E(\lambda_1,T_s)$ and $E(\lambda_2,T_s)$ measured by the photoactive sensor of CIT-1MD into equation (2), one can obtain T_s.

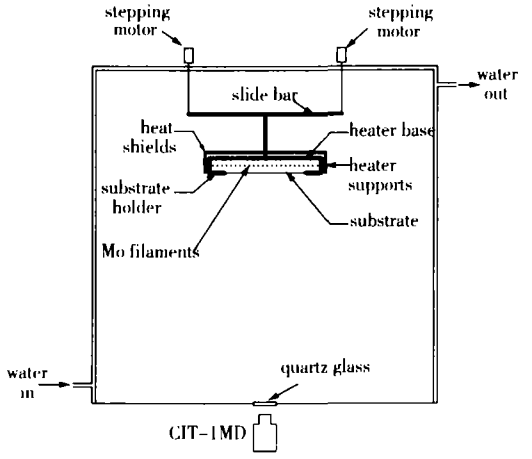

Fig. 1 Schematic diagram of our radiation heater in a vacuum chamber

3 Computational method of substrate temperature distribution

Under the vacuum condition, in the electronic beam physic vapor deposition (EB-PVD) process we are concerned about, the background pressure is about 10^{-3} Pa, and the convective HEAT FLUX can be neglected[16], so we just consider the radiative heat flux between the filaments and the radiative cavity and the effect of the thermal conduction on each part's temperature distribution.

In order to exactly simulate the radiative heat flux emitting from the molybdenum filaments' surface, every piece of molybdenum filaments is axially and circumferentially uniformly divided into 100×50 surface elements. The heat base is uniformly divided into 50×50 square surface elements, and every heat support around the radiative cavity is uniformly divided into 22×50 rectangle surface elements.

The radiative cavity's bottom surface made up of the substrate and its holder is uniformly divided into 50×50 square surface elements. For the surface element lying on the border of the substrate and its holder, if its center lies within the radius of the substrate, it will be treated as a substrate surface element, otherwise as a substrate holder surface element.

For the steadily-heating process we are interested in, any surface element n of the radiative cavity satisfies the energy balance equation which is of the form

$$q_{n,i}-q_{n,o}=q_{n,r}+q_{n,e}+q_{n,c} \qquad (3)$$

where q is the heat flux, subscripts i, r and e are the incident, reflective and emissive radiation respectively, o is the net radiative heat loss, and c is the thermal conduction.

3.1 Radiative heat flux of the radiative cavity inner-side

The incident radiative heat flux $q_{n,i}$ comes from the net emissive radiation of the

molybdenum filaments and the emissive and reflective radiation of other parts of the radiative cavity

$$q_{n,i} = \sum_{k=1}^{m} F_{k-n}\, q_{k,r} + \sum_{j=1}^{\ell} F_{j-n}\,(q_{j,r}+q_{j,e})\ (n\neq j) \tag{4}$$

where m is the total number of the surface elements of the molybdenum filaments, ℓ is the total number of the surface elements of the radiative cavity, F is the view factor, the former in subscripts $k-n$ and $j-n$ is the index number of the emissive surface elements, and the latter is the index number of the absorptive surface elements.

Generally speaking, the radiation characteristics of a nonmetallic surface are quite similar with those of a gray surface, so the silicon substrate surface can be treated as a gray surface. Because the vacuum radiation heater is time after time used under the condition of high temperature, especially in the in situ annealing process it is immersed in an abundant oxygen environment, a dense oxidable metal film will come into being on the surface of the stainless parts. These oxide films have similar radiation characteristics with those of a gray surface, so the inner and outer surfaces of the radiative cavity can be approximately regarded as gray surfaces.

According to the radiation characteristic of a gray surface,[17] the reflective radiative heat flux in equation (4) is written as

$$q_{j,r}=\beta_j q_{j,i} \tag{5}$$

where the reflective coefficient β_j is a constant which depends upon the property of the material surface. The reflective coefficients of stainless oxide film and silicon are 0.20 and 0.06 respectively.[18]

According to the Stefan - Boltzmann law,[17] the emissive radiative heat flux in equation (4) can be written as

$$q_{j,e}=\varepsilon_j\sigma T_j^4 A_j \tag{6}$$

where σ is the Stefan - Boltzmann constant, and ε_j, T_j and A_j are the emissive coefficient, the temperature and the area of surface element j respectively. For the gray body without transmission we are concerned about at present, $\varepsilon_j=1-\beta_j$, hereby the emissive coefficients of the stainless oxide film and the silicon substrate are 0.80 and 0.94 respectively.

The view factor F_{k-n} is defined as the fraction of the radiation leaving the surface element k that arrives at the surface element n. The symbol $d_{k,n}$ is the distance between these two surface element centers, and φ_k and φ_n are the included angels between the line across these two surface element centers and their own normal. If $\varphi_k \geqslant \pi/2$ or $\varphi_n \geqslant \pi/2$, $F_{k-n}=0$. If $0\leqslant\varphi_k,\varphi_n\leqslant\pi/2$, and $\cos\varphi_k dA_k \ll d_{k,n}^2$ and $\cos\varphi_n dA_n \ll d_{k,n}^2$, the view factor can be obtained[17]

$$F_{k-n}=\frac{\cos\varphi_k\cos\varphi_n A_n}{\pi d_{k,n}^2} \tag{7}$$

3.2 Net radiative heat flux loss of the radiative cavity

When the heating process of IMCAS - VRH in vacuum becomes stable, the net heat flux loss of the outer surface of the radiative cavity ought to be equal to the thermal conductive heat flux between its inner and outer surfaces. It is of the form

$$\gamma\varepsilon\sigma T^4\approx\kappa\Delta T/\delta \tag{8}$$

where δ is the thickness of the radiative cavity, ΔT is the temperature difference be-

tween its inner and outer surfaces, κ is the thermal conductive coefficient of the radiative cavity, γ is a constant depending on the number of the heat shields out of the radiative cavity.

For any two parallel gray plates whose emissive coefficients are both ε, with their temperatures being T_1 and T_2 respectively, if thin heat shields with the same gray characteristics are laid between them, the radiative heat flux can be written as[17]

$$q_{1-2}=\gamma\varepsilon\sigma(T_1^4-T_2^4) \quad (9)$$

where $\gamma=1/(\omega+1)$, ω is the number of heat shields.

Two pieces of heat shields are installed out of the heater base and the supports, correspondingly $\gamma=1/3$. There are no heat shields out of the substrate and its holder, so $\gamma=1$. At the typical heating temperature, 1100 K, the thermal conductive coefficients ($unit\ Wm^{-2}K^{-1}$) of silicon and stainless steel are about 15 and 35 respectively.[18] The temperature difference ΔT between the inner and outer surfaces of the 0.5mm - thick silicon substrate, calculated with equation (8) and (9), is approximately equal to 1 K, and ΔT of the 8mm - thick heater base, the heater supports and the substrate holder are approximately10 K, which are both far less than1100 K. Therefore the temperatures of the inner and outer surfaces of the whole radiative cavity are nearly the same.

RH is used in a vacuum chamber with a double - layer water - cooling wall (shown in Fig. 1). When the temperature of the outer surface of the radiative cavity T_o is about 1100 K, the temperature of the inner surface of the vacuum chamber, measured by thermocouple, T_v is about 400 K. According to equation (9), the net radiative transfer loss of the outer surface of the surface element n in equation (3) can be written as

$$q_{n,o}=\gamma_n\varepsilon_n\sigma(T_o^4-T_v^4)A_n\approx\gamma_n\varepsilon_n\sigma T_n^4A_n. \quad (10)$$

3.3 Net radiative heat flux of the Mo filaments and their shielding effect

The molybdenum filaments are the only positive heating sources, and the net radiative heat flux $q_{k,r}$ of the molybdenum filament surface element in equation (4) can be determined by the following iterating method. Take W_h as the steady electric heating power of RH, and assume all molybdenum filament surface elements have the same output power and the initial value $q_{k,r}=W_h/m$, we calculate the corresponding total radiative consumption power of the outer surface of the radiative cavity with the form

$$W_c=\sum_{n=1}^{\ell}\gamma_n\varepsilon_n\sigma T_n^4A_n. \quad (11)$$

If $W_c<W_h$, we increase $q_{k,r}$, or otherwise we decrease it, until $|1-W_c/W_h|\leqslant\varepsilon_h$. In our calculation, $\varepsilon_h=0.001$.

RH has 24 pieces of molybdenum filaments in all, and the sum area of the axial - direction section divided by the section area of the radiative cavity on the molybdenum filament axial plane is 0.36, so the shielding effect of the molybdenum filaments on radiation must be taken into account.

We build up a Cartesian coordinate system, in which the origin O is set in the center of the section of the radiative cavity in the molybdenum filaments' axial direction,

X axis vertically directs to the substrate surface, and Y axis and Z axis are vertical and parallel to the molybdenum filaments' axes respectively.

As for two surface elements 1 and 2 whose coordinates of central points are (x_1, y_1, z_1) and (x_2, y_2, z_2) respectively, their connecting line equation can be written as

$$\frac{x-x_1}{x_2-x_1}=\frac{y-y_1}{y_2-y_1}=\frac{z-z_1}{z_2-z_1} \tag{12}$$

If $x_1=x_2$, $y_1=y_2$ or $z_1=z_2$, equation (12) degenerates to $x=x_1$, $y=y_1$ or $z=z_1$. The following solution course can be correspondingly simplified.

The surface equation of one molybdenum filament with coordinates of the central point $(0, y_0, 0)$ and the radius r_f

$$x^2+(y-y_0)^2=r_f^2 \tag{13}$$

Through the simultaneous equations (12) and (13), one can obtain the intersectant point equation

$$Az^2+Bz+C=0 \tag{14}$$

where

$$A=\left(\frac{x_2-x_1}{z_2-z_1}\right)^2+\left(\frac{y_2-y_1}{z_2-z_1}\right)^2 \tag{15}$$

$$B=\frac{-2z_1[(x_2-x_1)^2+(y_2-y_1)^2]}{(z_2-z_1)^2}+\frac{2x_1(x_2-x_1)+2(y_1-y_0)(y_2-y_1)}{z_2-z_1} \tag{16}$$

$$C=\frac{z_1^2[(x_2-x_1)^2+(y_2-y_1)^2]}{(z_2-z_1)^2}+x_1^2+(y_1-y_0)^2-r_f^2 \tag{17}$$

If $\Delta=B^2-4AC<0$, the line has no intersectant point with the cylinder surface.

Now this molybdenum filament has no shielding effect on radiation between the surface elements 1 and 2. If $\Delta=B^2-4AC\geqslant 0$, the intersectant point coordinates of line (12) and cylinder (13) are

$$x_i=x_1+\frac{z-z_1}{z_2-z_1}(x_2-x_1)$$

$$y_i=\frac{y_2-y_1}{z_2-z_1}(z-z_1)+y_1$$

and $z_i=\dfrac{-B\pm\sqrt{B^2-4AC}}{2A}$. If $\min(x_1, x_2)<x_i<\max(x_1, x_2)$, $\min(y_1, y_2)<y_i<\max(y_1, y_2)$ $\min(z_1, z_2)<z_i<\max(z_1, z_2)$ and $-l_f/2\leqslant z_i\leqslant l_f/2$, this molybdenum filament has shielding effect on the radiative heat transfer of the surface elements 1 and 2, otherwise there is no shielding effect.

3.4 Effect of thermal conduction on temperature distribution

According to Fourier's law of heat conduction, $q_{n,c}$ in equation (3) is equal to the sum of conductive heat flux which transfers from the surface element n to another four circumambient surface elements. Take the bottom surface of the radiative cavity made up of the substrate and its holder for example, the expression for $q_{n,c}$ can be written as[19]

$$q_{n,c}=\kappa\delta\Delta y\frac{(T_{j,k}-T_{j,k+1})+(T_{j,k}-T_{j,k-1})}{\Delta z}+\kappa\delta\Delta z\frac{(T_{j,k}-T_{j+1,k})+(T_{j,k}-T_{j-1,k})}{\Delta y}, \tag{18}$$

where subscripts j and k are the indices of this surface element in the direction of Y and Z.

The substrate holder is hung on the heater barriers by three linking points, and the heater barriers and the heater base are connected by point jointing. The connecting surface of the substrate and its holder is very small, so the interfaces between any two parts of the radiative cavity can be treated as under the adiabatic boundary condition in the calculation.

3.5 Temperature calculation of the radiative cavity

Substituting the expressions for incident, emissive and reflective radiative heat flux, i. e. equations (4~6), the net loss of the radiative heat flux of the outer surface element, equation (10), and the thermal conductive heat flux, equation (18) into equation (3), thus one can obtain the energy balance equation of surface element n. This article uses the deepest descend method[20] to simultaneously resolve these energy balance equations of all surface elements. For the hypothetic initial temperature distribution of the radiative cavity, we will have a bran-new temperature distribution by calculating every radiative heat flux and every thermal conductive heat flux. We may perform this loop, until the sum of the absolute value of the temperature - change over all surface elements satisfies the given precision request.

In order to check the calculating program, we assume a perfect instance without molybdenum filaments: the initial temperature of the substrate with a diameter of 6 inches is 300 K, the temperatures of other parts are all the same T_0, and the outer surface of the radiative cavity are treated as under the adiabatic boundary condition. We calculate four conditions, T_0 = 800 K, 1000 K, 1200 K and 1400 K respectively. Under each condition, the theoretical temperatures of the substrate should convergence into and stabilize at T_0 correspondingly. The differences between the calculated and theoretical temperature value for the four conditions are all less than 0.16 K (shown in Fig. 2). The temperature of the peripheral region of the substrate is appreciably greater than that of the central region. This is because that the peripheral region is relatively close to the heat supports and the error of the calculated view factor is appreciably increasing. Generally speaking, the calculated results are satisfying and validate the veracity of the division of the surface elements and the calculating program at present.

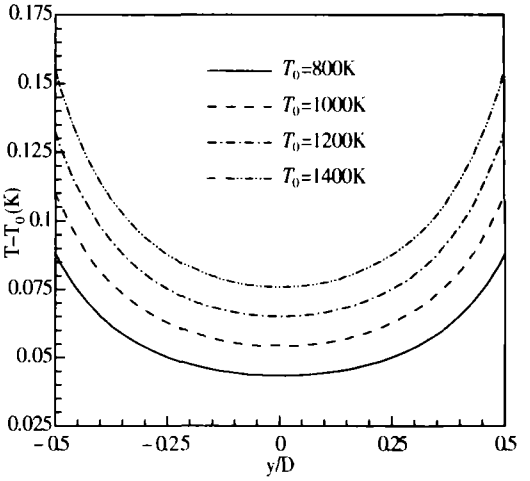

Fig. 2 The calculational temperature distribution of the substrate with a diameter of 6 inches under the perfect conditions

4 Comparison of calculated and metrical temperature distributions

Fig. 3 shows the comparison of the calculational temperature results with the experimental results of the substrate surface with a diameter of 6 inches under an electric power of 3860 W. The calculational temperature distribution agrees well with the metrical data. Compared with the average temperature of the substrate, namely 1093 K, the metrical temperature data of the central region are appreciably 2 K higher, and those

of the peripheral region are appreciably 4 K lower. The whole relative temperature distribution variation of the substrate is 5‰ only, which is satisfying.

Fig. 4～Fig. 7 reviews the effects of various factors on the temperature uniformity of the substrate surface. Firstly, the molybdenum filaments' shielding effect is shown. Four conditions are considered: i) there is shielding effect between the molybdenum filaments, and the molybdenum filaments have shielding effect on the radiative cavity; ii) there is no shielding effect between the molybdenum filaments, and the molybdenum filaments have shielding effect on the radiative cavity; iii) there is shielding effect between the molybdenum filaments, and the molybdenum filaments have no shielding effect on the radiative cavity; iv) there is no shielding effect between the molybdenum filaments, and the molybdenum filaments have no shielding effect on the radiative cavity. Fig. 4 compares the calculational temperature distribution of the substrate surface on the diameter, which is vertical to the molybdenum filament axial, and under these 4 conditions, the average temperature $\overline{T}$ of which are 1093 K, 1125 K, 1273 K and 1322 K respectively. It can been seen that due to the absence of shielding effect between the molybdenum filaments, the incident radiative heat flux under condition ii rises compared to condition i, which not only brings up the average temperature, but also increases the incident radiative heat flux of the peripheral region of the substrate and drives up the temperature difference correspondingly. Comparisons of conditions i - ii, i - iii, i - iv show that the shielding effect between molybdenum filaments is disadvantageous to the temperature uniformity of the substrate surface, while the shielding effect of the molybdenum filaments on the surface elements on the radiative cavity benefits the temperature uniformity. In all, the shielding effect of the molybdenum filaments is disadvantageous to the temperature uniformity of the substrate.

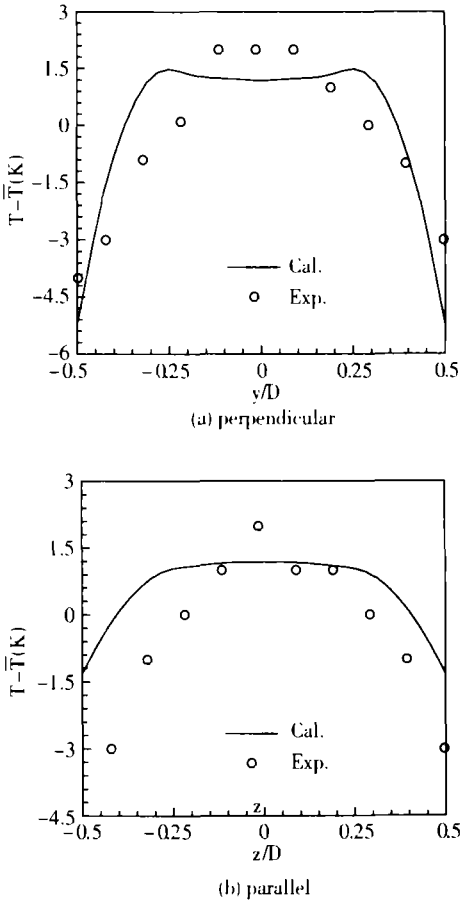

Fig. 3 Comparison of the calculated and metrical temperature distributions over a monocrystal silicon substrate with a diameter of 6 inches in vacuum along the perpendicular and parallel directions to the molybdenum filaments, respectively.

Fig. 5 reviews the effect of heat shields on the temperature uniformity of the substrate. $\gamma^* = 1/3$ corresponds to the practical condition, where there are two pieces of heat shields out of the heater base and the supports, and $\gamma^* = 1$ corresponds to the

given condition where there are no heat shields. The average temperatures $\overline{T}$ under these two conditions are 1093 K and 1049 K respectively. Under the given condition without heat shields, not only the average temperature over the substrate surface decreases 44 K, but also the uniformity of temperature distribution markedly descends. This is mainly because that the decrease of temperatures of the heater supports and the peripheral region of the heater base weakens the incident radiation on the peripheral region of the substrate surface more than that on the central area, and consequently debases the uniformity of temperature distribution of the substrate surface.

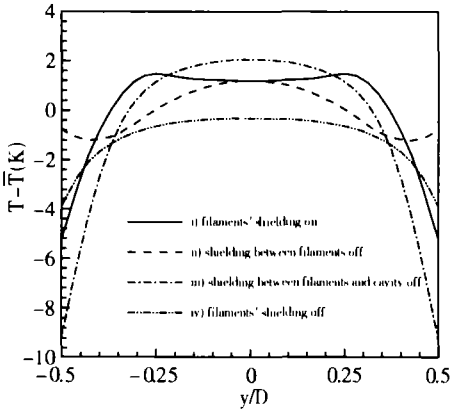

Fig. 4 The shielding effect of the molybdenum filaments on the substrate temperature distribution

Fig. 6 gives the comparison of the temperature distribution of the substrate surface under two conditions, namely the conditions under which the radiation of the heater base, the heater supports and the substrate holder are 'on' and 'off' respectively, and the corresponding average temperatures $\overline{T}$ are 1093 K and 945 K respectively. The qualitative contrast 'on' between 'off' is similar with Fig. 5, but the quantitative effect on the average temperature and the temperature uniformity is more severe.

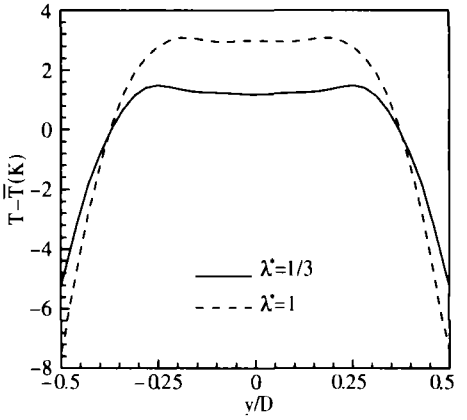

Fig. 5 The effect of the heat shields out of the heater base and the supports on the uniformity of temperature distribution of the substrate surface

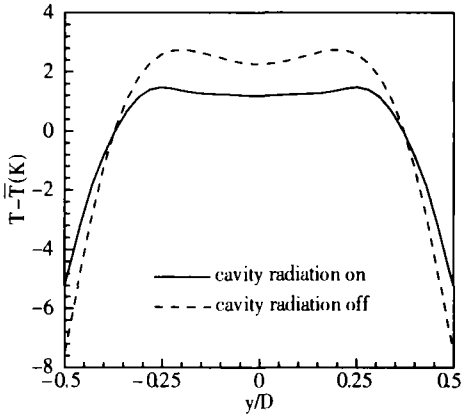

Fig. 6 The effect of the radiative cavity on the uniformity of temperature distribution of the substrate surface

Fig. 7 shows the effect of the thermal conduction in the radiative cavity on the temperature uniformity of the substrate surface. The average temperatures under the two conditions of considering and neglecting the thermal conduction are 1093 K and 1094 K respectively, the difference of which is very little. However, under the

latter condition the local temperature gradient over the peripheral region of the substrate surface in the nonuniformity of the incident radiative the molybdenum filaments' shielding effect results is comparatively larger. This is mainly because that heat flux of the substrate surface, and the thermal conduction can weaken or eliminate this nonuniformity to some extent.

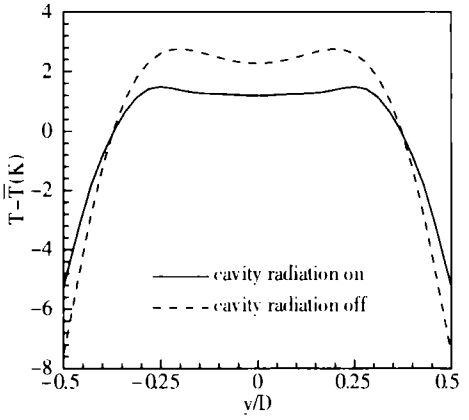

Fig. 7 The effect of thermal conductivity on the uniformity of temperature distribution of the substrate surface

5 Conclusions

This article analyzes, with the employment of numerical calculation and infrared colorimetric measurement of temperature, the performance of RH, the radiation heater used in vacuum we have designed and fabricated. When using RH to heat a monocrystal silicon substrate with a diameter of 6 inches under an electric power of 3860 W, the mean temperature of the substrate surface is 1093 K, and the temperature variation of the whole substrate is 6 K only. The uniformity of temperature distribution is satisfying.

The calculational results accord with the metrical data. Besides, we analyze the molybdenum filaments' shielding effect on radiation, the heat shields, and the thermal conduction of the radiative cavity through further calculational analysis. The present papers have partly or even completely neglected these factors for the convenience of analysis. However, our calculational results show that they significantly affect the temperature uniformity of the substrate, and should be considered in the optimal design of vacuum radiation heaters.

Acknowledgements

This work is supported by the Chinese Academy of Sciences and the National Science Foundation of China under grants 10205024 and 10502051. The authors are grateful to Dr. H. L. Liu and Mr. C. Xie for the careful calibration of the Pt/Rh - Pt thermocouple.

References

[1] I. C. J. Robbie, C. T. Stoddart, A substrate heater for use in the vacuum deposition of thin films. Journal of Scientific Instruments, 1: 56 - 57 (1968)

[2] 2. B. Oh, R. P. Robertazzi, Heater for high Tc oxide superconducting thin film deposition. , Rev. Sci. Instrum. 62(2): 3104 - 3105 (1991)

[3] 3. T. E. Jones, W. C. McGinnis, J. S. Briggs, Compact substrate heater for use in an oxidizing atmosphere, Rev. Sci. Instrum. 65(4): 977 - 800 (1994)

[4] 4. R. Campion, R. G. Ormson, C. A. Bashford, Design and performance of a reliable and low cost substrate heater for super-

conducting thin film deposition, Vacuum, 46 (2): 195 - 197 (1995)

[5] 5. H. Kinder, P. Berberich, B. Utz, D. Prusseit, Double Sided YBCO Films on 4" Substrates by Thermal Reactive Evaporation, IEEE Trans. Appl. Supercond., 5 (2): 1575 - 1580 (1995)

[6] 6. J. C. Clark, J. P. Maria, K. J. Hubbard, D. G. Schlom, An oxygen - compatible radiant substrate heater for thin film growth at substrate temperature up to 1050℃, Rev. Sci. Instrum. 68 (6): 2538 - 2541 (1997)

[7] 7. V. N. Tsaneva, V. I. Tsanev, E. J. Tarte, Z. H. Barber, F. Kahlmann, G. Gibson, M. G. Blamire, J. E. Evetts, Study of the radiative heating for deposition of high - Tc superconducting thin films, Vacuum, 58 :454 - 463 (2000)

[8] 8. J. Geerk, A. Zaitsev, G. Linker, R. Aidam, R. Schneider, F. Ratzel, R. Fromknecht, B. Scheerer, H. Reiner, E. Gaganidze, R. Schwab., A 3 - chamber deposition system for the simultaneous double - sided coating of 5 - inch wafers, IEEE Trans. Appl. Supercond., 11 (1): 3856 - 3858 (2001)

[9] 9. C. Liu, A. Macrander, Simple vacuum heater and its application for annealing TiO_2 films, J. Vac. Sci. Technol. A, 19 (5): 2703 - 2705 (2001)

[10] 10. J. J. Chen, B. W. Tao, X. Z. Liu, Y. R. Li, Some considerations on heater design for simultaneous deposition of large - area high - Tc superconducting thin films, J. Vac. Sci. Technol. A, 22 (2): 255 - 259 (2004)

[11] 11. R. Bellman, R. Raj, A tungsten filament high temperature heater for thin film deposition, Rev. Sci. Instrum. 67 (11): 3958 - 3960 (1996)

[12] 12. A. C. Westerheim, A. C. Anderson, M. J. Cima, Substrate temperature measurements using ultrasonically bonded platine II thermocouples, Rev. Sci. Instrum. 63 (4): 2282 - 2287 (1992)

[13] 13. A. C. Westerheim, B. I. Choi, M. I. Flik, M. J. Cima, R. L. Slattery, A. C. Anderson, Radiative substrate heating for high - Tc superconducting thin - film deposition: Film - growth - induced temperature variation, J. Vac. Sci. Technol. A, 10 (6): 3407 - 3410 (1992)

[14] 14. B. I. Choi, A. C. Anderson, A. C. Westerheim, M. I. Flik, In situ substrate temperature measurement in high - Tc superconducting film deposition, J. Vac. Sci. Technol. A, 11(6): 3020 - 3025 (1989)

[15] 15. G. Wagner, E. G. Gonzales, K. Numssen, and H. - U., Sputter deposition of large area Yba2Cu3O7 - δ thin films, Physica C 235: 637 - 638 (1994)

[16] 16. R. J. Visser, Determination of the power and current densities in argon and oxygen plasmas by in situ temperature measurements, J. Vac. Sci. Technol. A, 7: 189 - 194 (1989)

[17] 17. F. P. Incropera, D. P. DeWitt, Fundamentals of Heat and Mass Transfer, John Wiley & Sons, New York, 1996

[18] 18. L. T. Yeh, R. C. Chu, Thermal Management of Microelectronic Equipment, ASME Press, New York, 2002

[19] 19. D. R. Croft, D. G. Lilley, Heat Transfer Calculations Using Finite Difference Equations, Applied Science Publishers Ltd, London, 1977

[20] 20. A. L. Peressini, F. E. Sullivan, J. J. Uhl Jr, The Mathematics of nonlinear Programming, Springer - Verleg, NewYork, 1988